



Valuing Salt Marshes as Nature-based Infrastructure for Coastal Flood Mitigation: A Case Study of Chatham County, GA

Xinyu Zeng¹, Dede Long², Yukiko Hashida¹, Matthew V. Bilskie³

¹Department of Agricultural and Applied Economics, University of Georgia, Athens, GA 30601, USA

5 ²Department of Humanities, Social Sciences, and the Arts, Harvey Mudd College, Claremont, CA 91711, USA

³School of Environmental, Civil, Agricultural and Mechanical Engineering, University of Georgia, Athens, GA 30601, USA

Correspondence to: Yukiko Hashida (yhashida@uga.edu)

Abstract. Flooding poses significant economic challenges to coastal counties, affecting nearly 40% of the U.S. population. Nature-based solutions, also known as green infrastructure, are increasingly recognized as effective alternatives or complements to traditional gray infrastructure for flood risk mitigation. This study examines the flood damage reduction benefits of salt marshes, a key type of green infrastructure. We use physics-based spatially explicit hydrodynamic models to simulate storm scenarios and the resulting inundation depths with and without salt marshes. We then translate hydrological data into economic benefits by applying two distinct approaches, one based on the traditional US Army Corps of Engineers depth-damage function and another with an estimated depth-damage function derived from the National Flood Insurance Program (NFIP) claims data. Applying our integrated approach to the case study area, Chatham County in Georgia, we find that salt marshes contribute to significant damage reductions, ranging from \$30 million to \$40 million for a storm representative of the 1% annual exceedance probability event. This study offers policymakers valuable insights into implementing flood mitigation strategies through marshland conservation. Our integrated modeling framework is readily adaptable to coastal regions worldwide where salt marshes or similar coastal ecosystems provide flood-mitigation services.

20 **1 Introduction**

Tropical cyclone-driven flooding can pose a substantial burden on coastal counties, which are home to approximately 129 million people in the U.S., nearly 40% of the nation's population (NOAA, 2026). As the most common and costly natural disaster, coastal flooding causes greater economic losses and damage than any other severe weather event. In 2020, average annual flood damages reached \$32.1 billion, with projections indicating further increases due to the compound effects of rising sea levels, ocean warming (Wing et al., 2022), a growing population, and rapid urbanization (Cutter et al., 2018). As a result, substantial investments have been made in gray infrastructure, such as levees, dikes, floodwalls, dams, and reservoirs, to mitigate flood risks within vulnerable communities.

Recently, "nature-based solutions", also known as green infrastructure, have gained traction as alternatives or complements to traditional gray defensive infrastructure in flood risk mitigation. Natural coastal ecosystems (e.g., salt marshes, mangroves, barrier islands) can reduce flood risk, attenuate storm surge and waves (Spalding et al., 2014), and aid in



reducing stormwater runoff (Arkema et al., 2013; Narayan et al., 2017; Rezaie et al., 2020). While the physical benefits of coastal ecosystems are evident, translating these effects into economic benefits is crucial for conducting benefit-cost analyses (BCAs) and setting effective mitigation and risk-reduction goals. Previous research has primarily focused on quantifying the avoided damages from storm protection provided by coastal wetlands at the global (Costanza et al., 2021) and the regional level (Narayan et al., 2017), as well as avoided damages from hurricanes and tropical cyclones (Sun and Carson, 2020) and property protection (Farber, 1987). Taylor & Druckenmiller (2022) extended this research by empirically quantifying the flood mitigation benefits, focusing on inland wetlands instead of coastal wetlands.

However, for coastal protection, previous studies primarily focused on the wave attenuation effects in specific coastal habitats, including coral reefs (Ferrario et al., 2014), salt marshes (Möller et al., 2014), mangroves (Guannel et al., 2015), and marshes and levees (van Zelst et al., 2021). The monetary value of property flood-mitigation benefits provided by different types of coastal wetlands remains understudied and poorly understood. This paper addresses this gap by integrating a hydrodynamic model into an econometric analysis to examine the flood-damage-reduction benefits of salt marshes. We first simulate overland coastal flooding from synthetic storm tracks using high-resolution spatially explicit computational hydrodynamic models. These simulations project the counterfactual scenarios in inundation levels with and without salt marshes, illustrating how marsh vegetation influences water depth during storms. Using simulated water depths, we estimate the change in annual flood damages attributable to marshes and how these impacts are distributed, with a specific focus on differences in benefits between disadvantaged populations (low-income and minority-dominant) and their counterparts.

To translate the physical flood reduction benefits of marshes into economic terms, we rely on depth-damage relationships. Following previous studies, we utilize the standard depth-damage function developed by the U.S. Army Corps of Engineers (USACE), a widely used off-the-shelf depth-damage function for flood risk assessments both nationally and globally. As an alternative to this traditional approach, we also employ an empirical, data-driven method, estimating a depth-damage function using a rich dataset of flood claims from the National Flood Insurance Program (NFIP), maintained by the Federal Emergency Management Agency (FEMA). Estimating flood damage using both methods enables us to compare the standard USACE approach with the outcome based on empirical insurance claim data. We then predict property damage associated with inundation scenarios, both with and without salt marshes, using parameters obtained from the separate sets of depth-damage functions. We apply this integrated hydrodynamic and economic approach to Chatham County, Georgia. With various areas of the county located within low-lying coastal plains, Chatham County is particularly vulnerable to storms and flooding (Chatham County Department of Engineering, 2025). This vulnerability has led to government agencies and non-governmental organizations investing in marshland conservation to improve coastal resilience against climate challenges (Chatham County, 2026). We estimate both the total avoided damage from salt marshes and the distribution of these benefits across communities with varying socioeconomic characteristics in Chatham County.

This paper makes several contributions to existing literature. First, by integrating hydrodynamic analysis with economic depth-damage functions, we translate the water-level attenuation effect of salt marshes into economic benefits and examine the spatial distribution of avoided damage across disadvantaged populations. Salt marshes, among the most fertile coastal



65 habitats, play a significant role in flood mitigation and adaptation, especially in low-lying coastal areas vulnerable to sea
level rise (Gedan et al., 2009; Shepard et al., 2011). In response to increasing coastal vulnerabilities, many regions exposed
to flood risks have implemented marsh conservation programs to improve resilience to natural disasters. For example, in
Georgia, the Coastal Marshlands Protection Act of 1970 and the Shore Assistance Act of 1979 were implemented to
conserve marshlands that provide crucial flood protection and habitat support (Bolster, 2020).

70 Second, using rich NFIP claims data, we estimate a data-driven depth-damage function and verify the robustness of the
conventional USACE depth-damage function. Wing et al. (2020) highlight the validity of using the observed flood losses
from the NFIP database to infer the depth-damage relations. They do so by analyzing the empirical distributions of median
relative damage (i.e., structural damage as a percentage of building value) and flood depth. We expand this approach by
estimating a non-linear depth-damage function. Additionally, while Wing et al. (2020) focus only on buildings with one
75 story and no basement, we expand the building types to residential homes with up to three stories, with and without a
basement. More importantly, we extend their approach beyond projecting flood damage to further quantify the flood-
damage-reduction benefits of salt marshes.

2 Methods

2.1 Methods Overview

80 Figure 1 presents a flowchart that outlines our method for assessing the effects of salt marshes on coastal flooding and
residential building damage. Our approach begins with a computational hydrodynamic model. The hydrodynamic model
simulates the water-level response to a tropical cyclone, and the results provide inundation depth and extent for scenarios
with and without coastal marsh vegetation. NFIP claims data are used to estimate a depth-damage function, where the
dependent variable is relative damage, defined as the ratio of structural damage to building value. Using the NFIP-derived
85 and USACE depth-damage functions and building structure data from the National Structure Inventory (NSI) and Chatham
County property records, we predict flood damages in Chatham County, Georgia, for both scenarios: with and without
marshes. The difference in damage represents the mitigation benefits that coastal salt marsh vegetation provides. Finally, to
examine the spatial distribution of these benefits, we overlay census block-level socioeconomic data with the projected
mitigation outcomes.

90

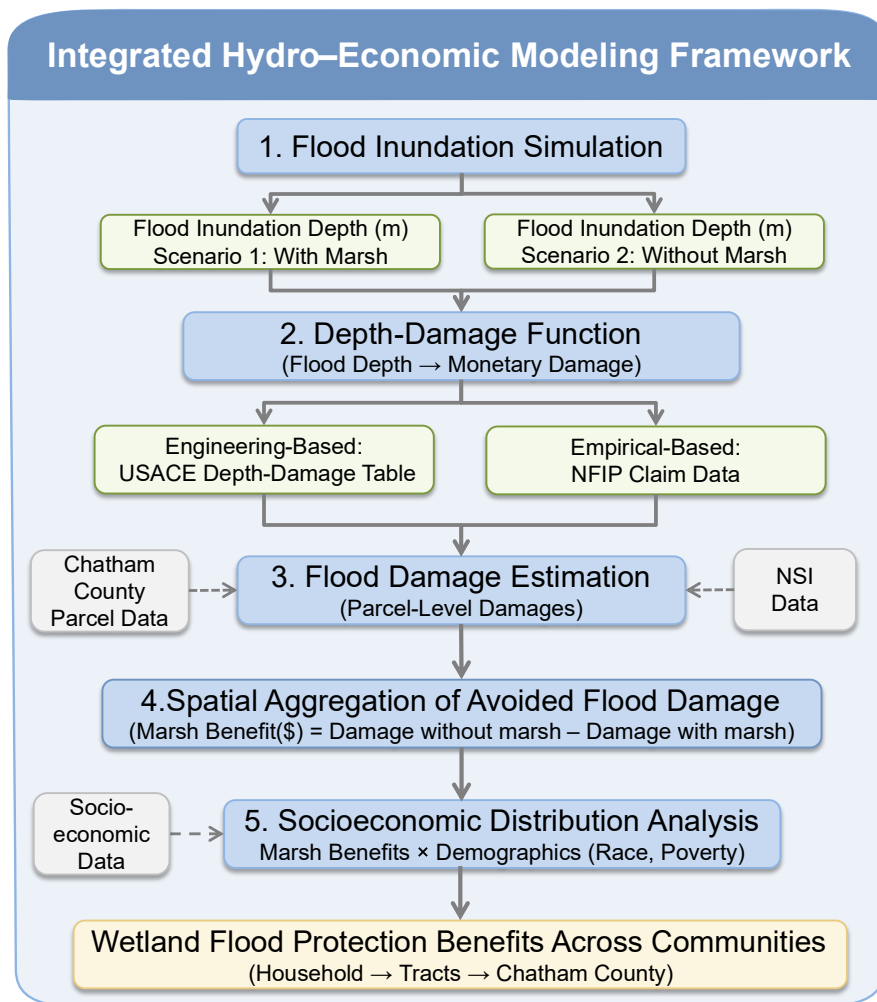


Figure 1: A Flow Chart Outlining the Methods.

In the following sections, we describe the hydrodynamic simulations (Section 2.2), the USACE depth-damage function approach (Section 2.3), the NFIP data-based depth-damage function approach (Section 2.4), and integration of these depth-damage functions with parcel-level and building inventory data (Section 2.5) in detail.

2.2 Hydrodynamic Simulations

We simulate storm water levels and wave dynamics from tropical cyclones using the ADvanced CIRCulation (ADCIRC) model, coupled with the Simulating WAVes Nearshore (SWAN) model (Dietrich et al., 2011). The coupled ADCIRC+SWAN framework is implemented on the unstructured mesh developed for the USACE South Atlantic Coastal Study (SACS), which spans the southeastern US coastline. The mesh extends across the western North Atlantic and provides



a resolution of up to 50 meters in nearshore areas along the southeastern coast. This high resolution enables detailed representation of coastal bathymetry and topography within the study area, as illustrated in Figure 2 for the study area.

This modeling system is widely used to evaluate coastal flood hazards and has been applied extensively in regional flood risk assessments.

105

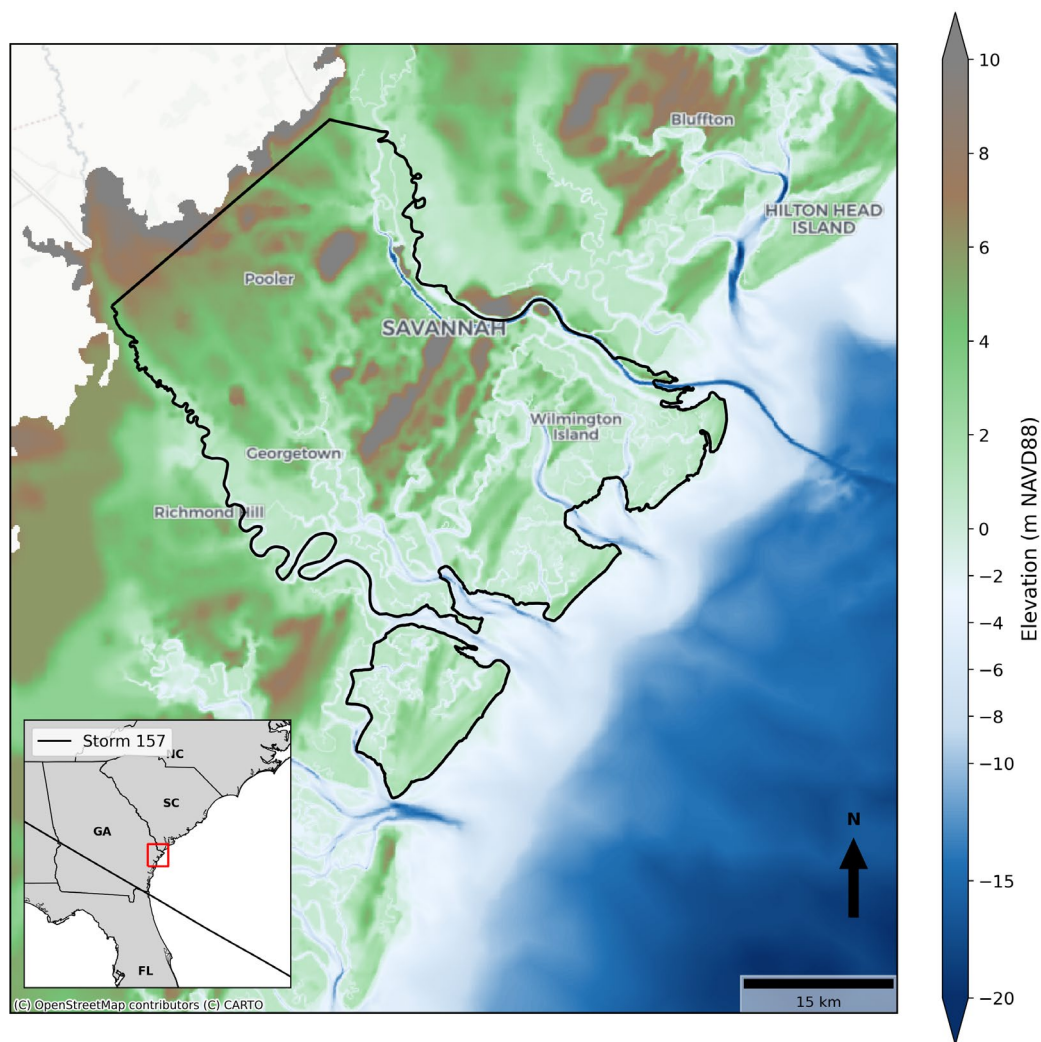


Figure 2: ADCIRC+SWAN model mesh topography and bathymetry (m, NAVD88) for the northern coast of Georgia. Chatham County is outlined in black.

ADCIRC solves generalized wave continuity equation (GWCE), to compute water surface elevation and depth-averaged velocity (Luettich and Westerink, 2004; Westerink et al., 2008). We run the model in two-dimensional, depth-averaged barotropic mode with a semi-implicit time-stepping scheme. A 2-second time step was adopted to ensure numerical stability and accurately capture the wetting and drying of elements. Advective terms were enabled, and a Smagorinsky-type turbulence closure scheme was used with a value of 0.2. A minimum bottom friction coefficient of 0.0015 was employed.

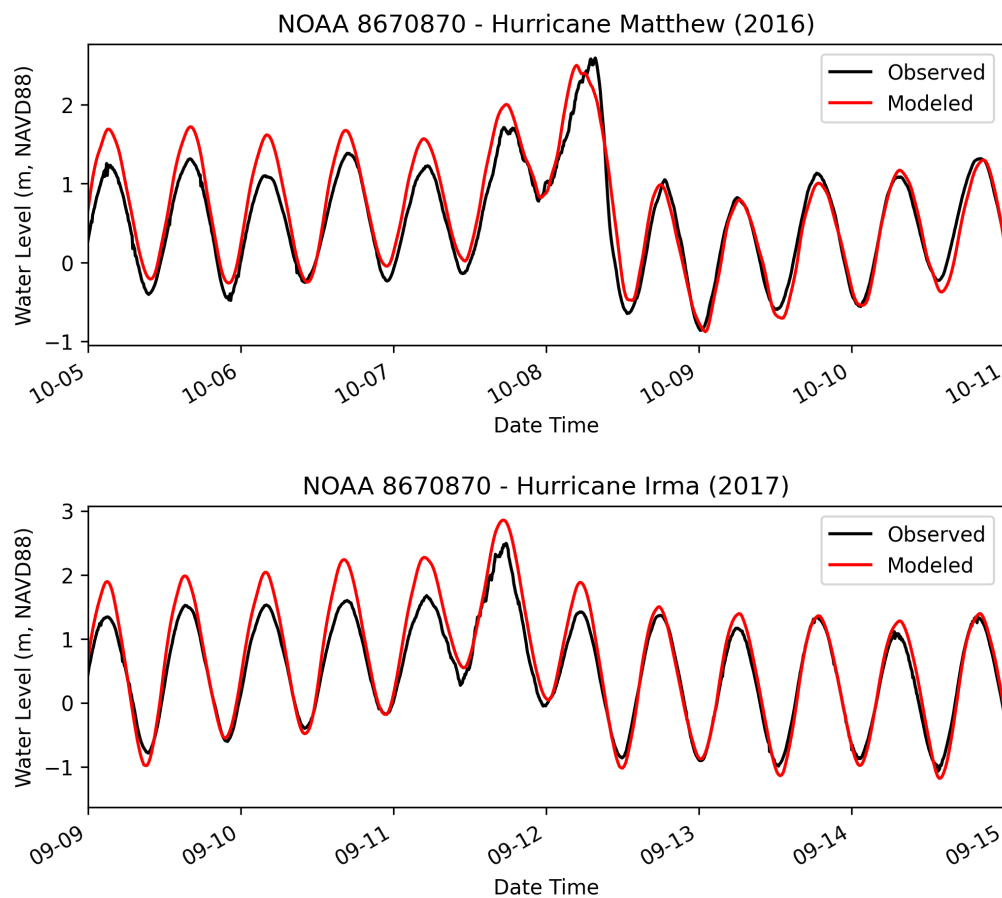


Wind drag was computed using the Powell wind-drag formulation with a maximum wind drag coefficient of 0.003.
115 Manning's n bottom roughness and wind reduction factors were applied to reduce marine-based wind speeds due to land roughness (USACE, 2022).

SWAN simulates wind-generated waves by solving the spectral action balance equation and representing wave energy as a phase-averaged spectrum (Dietrich et al., 2011). The wave spectrum was discretized into 40 logarithmically spaced frequency bins ranging from 0.031 to 1.42 Hz and 36 directional bins with 10° resolution. The model includes standard
120 parameterizations for key physical processes: whitecapping following Komen (1984), wind-wave growth based on Cavaleri & Rizzoli (1981), bottom friction (with roughness values passed from ADCIRC) parameterized according to Madsen et al. (1988), and depth-induced breaking following Battjes and Janssen (1978).

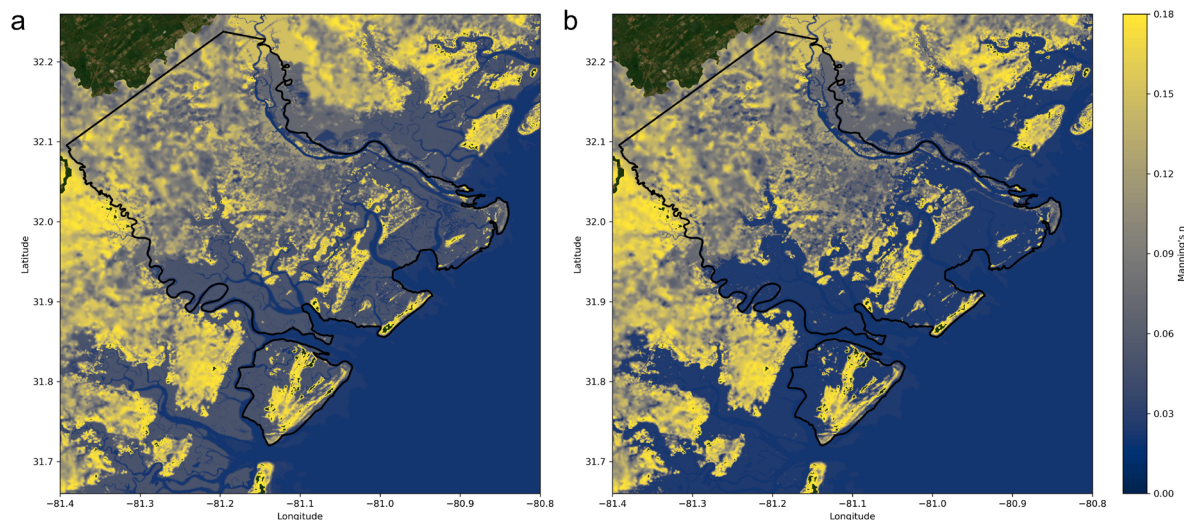
The model was configured to use a maximum of 20 iterations per time step. Convergence was achieved when at least 95% of grid points satisfied absolute and relative error tolerances of 0.005 and 0.01, respectively, and when the spectral curvature
125 change was less than 0.005. The time step was set to 1200 seconds, matching the ADCIRC+SWAN coupling interval. At each coupling interval, SWAN transmitted wave radiation stresses to ADCIRC, and ADCIRC returned updated water levels and current velocities to SWAN.

The modeling framework has previously been validated against historical tropical cyclone events, including Hurricane Matthew (2016) and Irma (2017) (Massey et al., 2025). Simulated water level time-series show strong agreement with
130 observations at the Fort Pulaski, GA, NOAA tide gauge (8670870), located near the study site (Figure 3). It accurately reproduces both the peak water level and timing for both storm events. A comprehensive validation across the entire model domain and additional tropical cyclones is provided in Massey et al. (2025). Here, we report only the validation results relevant to the present study for conciseness.



135 **Figure 3: Observed and ADCIRC modeled time-series water levels for Hurricane Matthew and Irma at the Fort Pulaski, GA NOAA gauge (8670870) in the Savannah River.**

To isolate the hydrodynamic contribution of marsh vegetation, we adjust the original model inputs by reducing the bottom roughness (Manning's n) within mapped marsh areas, treating them as open water to simulate “no marsh vegetation” conditions. The marsh platform elevations were held constant. Generally, short-term vegetation damage occurs without
140 accounting for alterations in marsh elevation (Figure 4). Storm surge-driven waves and inundation can lead to vegetation loss (Fagherazzi et al., 2013), edge erosion (Leonardi and Fagherazzi, 2015), and the formation of interior ponds (Castagno et al., 2021; Morton and Barras, 2011). Although storm-driven sediment deposition can occur, it is often temporary and may even enhance vegetation recovery when deposition thickness remains below approximately 5–10 cm (Walters & Kirwan, 2016).



145 **Figure 4: Manning’s n (bottom roughness) that represents a) current marsh vegetation and b) no marsh vegetation for Chatham County.**

Our objective is to recreate the 1% annual exceedance probability (AEP) stillwater floodplain (i.e., the 100-year return period) and evaluate the effects of reducing Manning’s n on total water levels, as described previously. The original SACS study utilized 1,700 synthetic storms across the southeastern U.S. coastline (including both Atlantic and Gulf coasts) to derive flood levels for various AEPs using Joint Probability Method with Optimum Sampling (JPM-OS). Because our analysis focuses on Chatham County, it was not necessary to simulate the full 1,700 storm set (USACE, 2022). Instead, we selected a subset of synthetic storms from the USACE storm database that produced peak water levels representative of the 1% AEP stillwater level for the Savannah–Chatham County area, defined as 3.75 m NAVD88. Storm 157 was chosen for simulation because it closely reproduces both the target 1% AEP stillwater level and has a representative storm track and storm parameters for the region (see the inset box of Figure 2 and Table 1). One additional storm was simulated to assess robustness; its parameters are available in the Appendix Table A1.

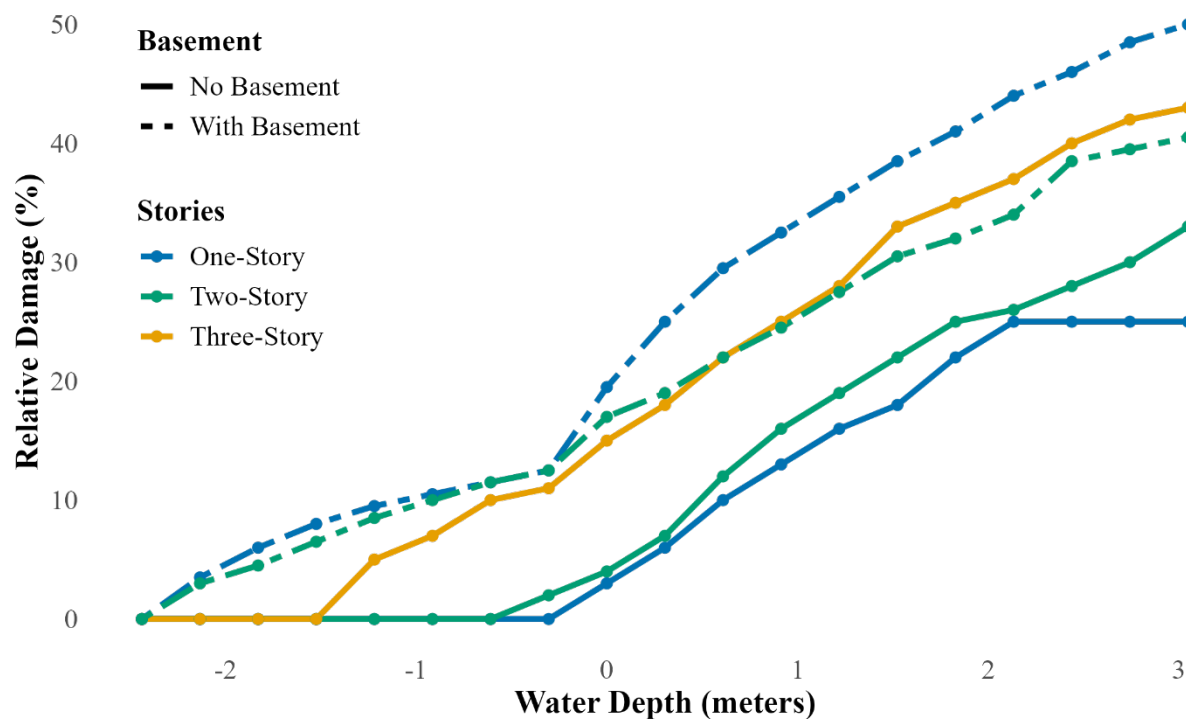
Table 1: USACE SACS storm track parameters for storm 0157.

Storm ID	Storm Heading (deg)	Central Pressure Deficit (hPa)	Radius of Maximum Winds (km)	Translational Speed (km/h)
0157	-60	68	117.3	28.9



160 2.3 USACE Depth Damage Function Approach

We adopt the USACE depth-damage function as our first approach to estimate flood damage. The USACE constructed the depth-damage function iteratively beginning in 1970, based on early NFIP loss data, local Army Corps studies, post-flood surveys, and expert input (Davis and Skaggs, 1992). These functions delineate the relationship between flood depths and losses, expressed as a percentage of building values (FEMA, 2020), as illustrated in Figure 5. They are commonly employed to predict building damage from flooding by returning the average percentage of expected structural and content loss for a given flood depth.



170 **Figure 5: USACE depth-damage functions for different occupancy types, categorized by the number of stories and the presence of a basement in the South Atlantic Division, Charleston District (Davis and Skaggs, 1992). Relative damage (%) is calculated as the ratio of damage to total property value. Water depth is measured in meters.**

2.4 NFIP Claim-Based Depth-Damage Function Approach

As an alternative approach, we estimate a non-linear depth-damage function using NFIP claims data, enabling us to compare estimated flood damage between the two methods. The NFIP, established by FEMA and created through the National Flood Insurance Act of 1968 (P.L. 90-448), serves as the predominant source of flood coverage for homeowners and has two purposes: to share the risk of flood losses through flood insurance and to reduce flood damage by restricting floodplain development (Horn and Webel, 2025). Today, more than 95% of the current residential flood policies sold are purchased through the NFIP (Kousky et al., 2023). We obtained approximately 2.5 million NFIP flood damage claims from 1978 to



2023 through the OpenFEMA Dataset: *FIMA NFIP Redacted Claims – v2*, where each claim record represents an insurance claim on a property that is located within FEMA’s Special Flood Hazard Area (SFHA) and for which there is an active NFIP policy.

As noted in Wing et al. (2020), a few anomalies are present in the claims data. First, the unit of flood depth is inconsistent: for some claims, it is recorded in inches instead of the standard unit of feet. This inconsistency is particularly problematic for claims with a flood depth of 6, as it is difficult to distinguish between 6 inches (half a foot) and 6 feet. Additionally, flood depths for some claims are recorded with multiples of 12 (e.g., 12, 24, etc.). We follow Wing et al. (2020) and restrict our sample to claims with depths of 8 feet or less to minimize measurement errors. Furthermore, to ensure consistency between the USACE depth-damage function and our estimated depth-damage function using NFIP data, we restrict our sample in several ways. Details are included in Appendix C.

Each claim entry contains the property’s location (latitude and longitude of the impacted building), the year the loss occurred, building damage, building value for each impacted residential building documented in the insurance claim, and inundation depths. Due to privacy protections applied to the public dataset, geographic coordinates are reported with a precision of two decimal places, corresponding to an approximate spatial resolution of 1.1 km (0.68 miles). We limit our sample to claims for the US East Coast, as these regions are susceptible to storms and flooding, and provide a comparable sample for estimating the depth-damage relationship used for our case study. Table 2 presents summary statistics for the main variables used to estimate the NFIP-derived depth-damage function. The average flood depth is about 0.65 meters, and the average relative structural damage is 20%. About 30% of the properties in the sample have finished basements, enclosures, or crawlspaces.

Table 2. Summary Statistics for Variables Used in Estimating the NFIP-Derived Depth-Damage Function

Variable	N	Mean	St. Dev.	Min	Max
Relative Damage (%)	232,790	0.20	0.23	0.00	1.00
Water Depth (meter)	232,790	0.65	0.50	0.3	2.44
Number of Floors	232,790	1.85	0.90	1.00	6.00
With Finished Basement	209,134	0.29	0.45	0.00	1.00

Unlike the USACE depth-damage approach above, which provides predetermined relationships between water depth and property damage, we need to infer the relationship from empirical claim data that records water depth and damage. Given the bounded nature of the relative damage—ranging from no relative damage (0%) to complete loss (100%)—we estimate a fractional logistic regression following Papke and Wooldridge (1996) to predict flood damage probability as a function of water depth and building structure type. This method is particularly adept at handling dependent variables, such as proportions or probabilities, that are constrained within a specific range. By controlling for building structures in addition to



water depth, our results predict flood damage for a given building structure and inundation depth, similar to the USACE method. As a robustness check, we also estimate the depth-damage function using beta regression. The beta regression results are presented in Appendix D.

Our fractional logistic regression model specifies the conditional mean via a logit link:

$$210 \quad \text{logit}(\mu_i) = \log\left(\frac{\mu_i}{1-\mu_i}\right) = \beta_0 + \beta_1 \text{WaterDepth}_i + \beta_2 \text{Floors}_i + \beta_3 \text{Basement}_i, \quad (1)$$

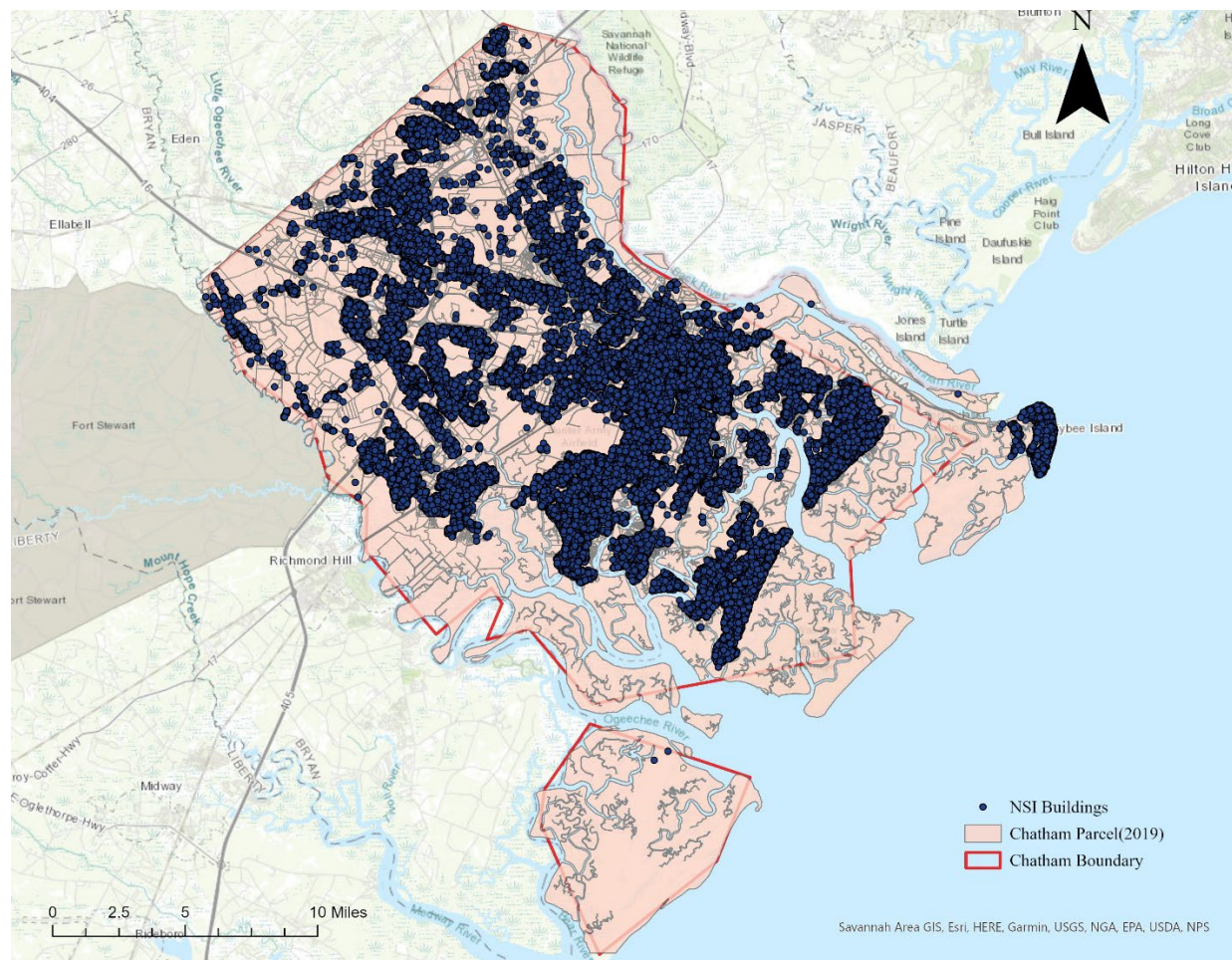
where $\mu_i = E(y_i|X_i)$ and y_i is the relative damage for property i , capturing structural damages as a percentage of building value (building damage divided by overall property value). WaterDepth_i is measured in meters, which is the main variable of interest. Floors_i indicates the number of floors, and Basement_i equals 1 if the property has a basement, 0 otherwise. The coefficients β_1 captures how increases in water depth change the log-odds of the flood damage fraction.

215 The marginal effects of flood inundation depth on the relative damage can be calculated as $\frac{\partial \mu_i}{\partial \text{WaterDepth}_i} = \mu_i(1 - \mu_i)\beta_1$. In addition, we estimate an alternative model by including the interaction terms between WaterDepth_i , Basement_i , and Floors_i to account for the heterogeneous effect of water depth on relative damage by building structures.

2.5 Combining depth-damage functions with Chatham County Parcel Data and the National Structure Inventory (NSI) data

220 After obtaining the depth-damage functions, we apply these functions to the property values based on the county parcel data combined with structure-specific characteristics to project the flood damages with and without marshes in the study region, Chatham County, Georgia. Figure 6 illustrates the spatial integration of county parcel data with NSI building locations used in the flood damage estimation process. To facilitate the projection, we obtained the 2019 parcel-level data for Chatham County from the Chatham County Savannah Area Geographic Information Systems open data site. The data provides
225 information on parcel boundaries, size, sales price, and land and real estate value.

Since the USACE and NFIP-derived depth-damage functions are specific to different building types, accounting for factors such as the number of floors and the presence of a basement, we spatially join the parcel-level building footprint in Chatham County with structural characteristics, including foundation height, number of stories, and presence of basement, obtained from the National Structure Inventory (NSI) (USACE, 2022). The NSI, maintained by the USACE, is a comprehensive
230 database that details the exposure and vulnerability of structures and is used in assessments of natural and man-made hazards and in planning for risk mitigation across the US. Each entry in the NSI corresponds to a single structure and provides detailed structural information. The above-ground foundation height is subtracted from the inundation depth of the simulated storm raster data. The number of stories and the presence of basement information in the NSI data enable us to estimate avoided damage in our case study region.



235

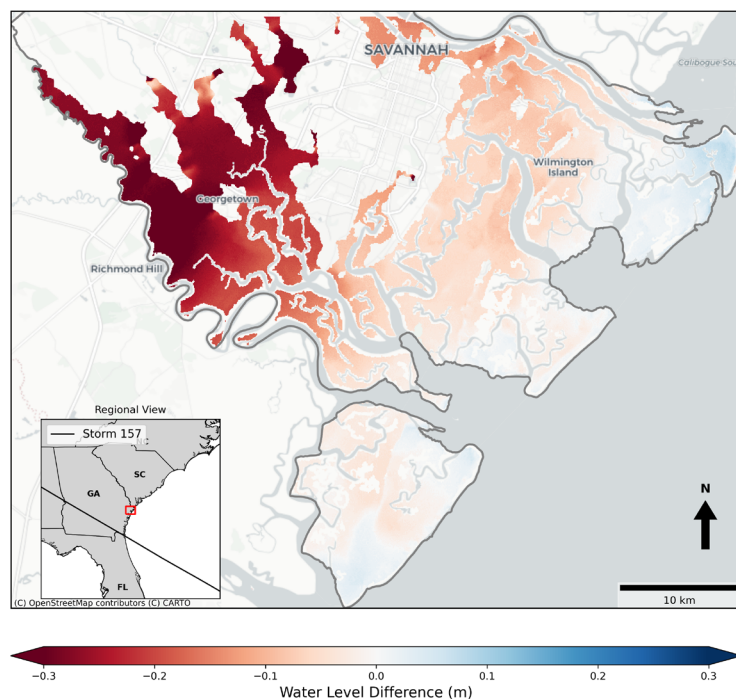
Figure 6: Chatham County Parcel Level Data Overlaid with the NSI Building Structure Data. The red outline indicates the boundary of Chatham County, while the pink baseline polygon represents the parcel data. The blue points indicate the locations of properties in the NSI data.

3 Results

240 3.1 Simulated Water Depths

Figure 7 illustrates the impact of salt marshes on flood depth and extent of storm 0157. Warmer colors indicate areas where marsh vegetation substantially reduces peak water levels, while cooler colors indicate regions where marshes slightly increase flood depths. Across much of Chatham County, flood depths decrease by up to 0.30 meters. The greatest reductions occur along the Ogeechee River near Georgetown. Other regions, including areas near Savannah, also experience reductions, though typically around 0.1 meters. While there are a few locations where the salt marsh vegetation raises water levels, these increases are negligible (less than 0.05 m).

245



250 **Figure 7: Change in water level (m) caused by marsh vegetation for synthetic storm 0157. Negative values indicate that marsh vegetation reduces peak water levels, while positive values indicate that it increases water levels. Chatham County, GA, is outlined in gray.**

3.2 Estimation Results of NFIP-Derived Depth-Damage Function

Table 3 presents the results of the fractional logistic regression used to estimate the NFIP-derived depth-damage function. In a logistic regression, coefficients represent changes in the natural log of the odds of the outcome. Therefore, our focus here is on the sign and significance of the parameter estimates. As expected, estimated positive coefficients for water depth in all four specifications indicate that relative damage is positively correlated with water depth, suggesting that damage increases with water depth on average. The results are robust across all specifications, with the damage associated with a one-meter rise in water depth being highest when two- and three-way interactions between the covariates are included.

To understand the magnitude of water depth's impact on relative flood damage (% of home values damaged), we calculate the average marginal effect of water depth. The marginal effects indicate that a 1-meter increase in water depth is associated with about a 6 percentage-point increase in relative damage.

265



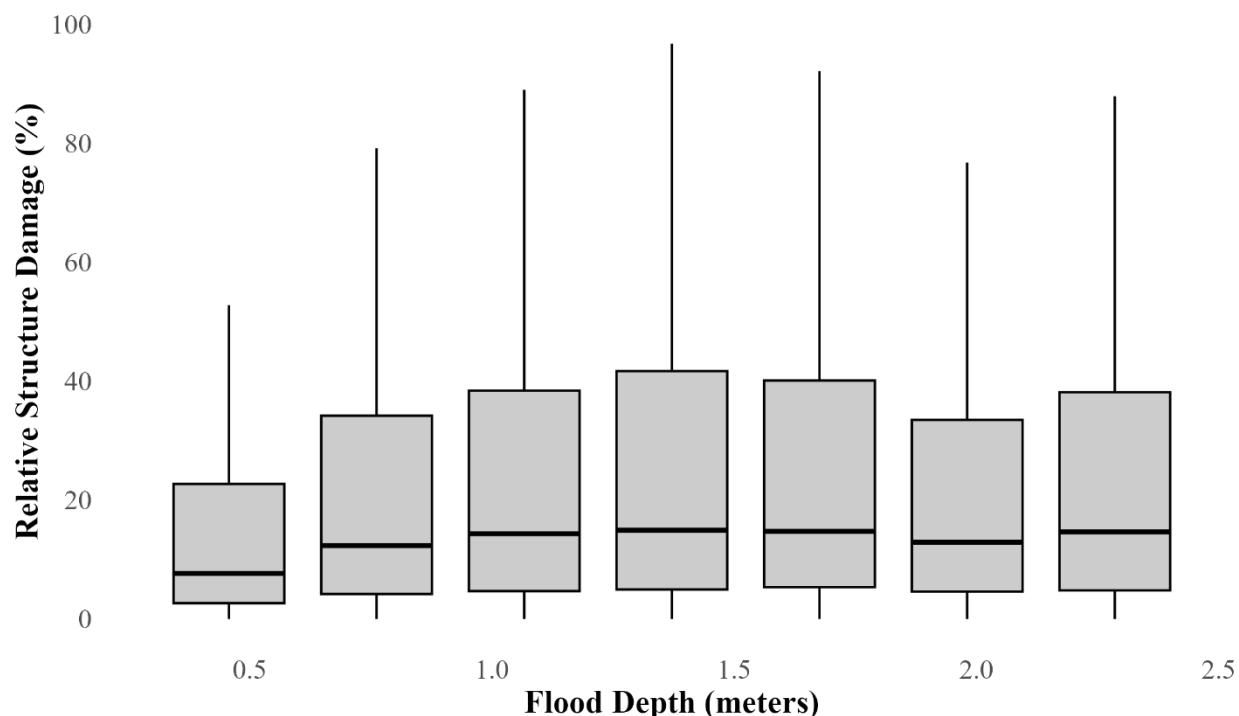
Table 3: Fractional logistic regression results with robust standard errors. The dependent variable is relative flood damage.

	(1)	(2)	(3)	(4)
Water Depth (m)	0.363*** (0.006)	0.384*** (0.006)	0.404*** (0.006)	0.570*** (0.019)
Number of Floors		-0.163*** (0.004)	-0.101*** (0.005)	-0.051*** (0.009)
With Basement			-0.432*** (0.009)	-0.053 (0.039)
Interaction with “Number of Floors” and “With Basement”	No	No	No	Yes
Marginal effect:				
Water Depth (m)	0.058*** (0.001)	0.061*** (0.001)	0.063*** (0.001)	0.065*** (0.001)
Observations	232,790	232,297	209,124	209,124
QAIC	64701.4	63826.8	62896.8	62781.6
R ²	0.0165	0.0309	0.0421	0.0440

Notes: This table presents the estimation results of the NFIP-derived depth-damage function using a fractional logistic regression. Robust standard errors are in parentheses. Significance denoted by * $p < 0.1$; ** $p < 0.05$; *** $p < 0.01$.

270

Figure 8 displays the NFIP-derived distribution of relative structural damage at each flood-depth increment for residential buildings with up to 3 stories. As mentioned in the method section, abnormalities in damage at a depth of 2 meters (around 6 feet) are likely due to measurement inconsistencies in the NFIP data.



275

Figure 8: NFIP-derived Depth-Damage Function for the East Coast Region

Notes: This figure presents the NFIP-derived depth-damage function. The boxplots illustrate the distribution of NFIP-derived relative structural damage (building damage divided by overall property value) at each increment of flood depth for residential buildings with up to three stories. The whiskers indicate the minimum and maximum values, while the shaded box is bounded by the 25th and 75th percentiles, with medians (50th percentile) inside. The claims data for the East Coast region, including Maine, New Hampshire, Massachusetts, Rhode Island, Connecticut, New York, New Jersey, Delaware, Maryland, Virginia, North Carolina, South Carolina, Georgia, and Florida, are used to estimate the depth-damage function. As a robustness check, we also include Washington DC, Pennsylvania, and Vermont in the sample and re-estimate the model, finding no meaningful difference in the results.

280

285 3.3 Predicted Benefits of Salt Marshes

Using NFIP-derived and USACE depth-damage functions merged with property data, along with simulated water depths from the hydrodynamic model, we quantify the avoided damage from salt marshes, measured as the difference between storm-induced flood damage with and without marsh vegetation. We focus our discussion on the predicted benefits of marshland based on storm track 0157, which represents the most likely storm path for our study area. Results for the alternative simulated storm track (storm 1313) are available in the Appendix Table A2.

290

Table 4 presents the aggregate and average mitigation benefits per household using the USACE and NFIP-derived depth-damage functions with and without interaction between water depth and other covariates (number of floors and basement). The average flood damage per claim was \$19,022 in Chatham County and \$27,177 nationwide, according to the NFIP data over the last 40 years. This indicates that salt marshes' flood damage mitigation benefits, about \$2,000 per storm per house,



295 equal about 10.5% of the average flood damage recorded in the past across homes in Chatham County. This totals
 approximately \$30 million for Chatham County, calculated by multiplying \$2,000 by approximately 15,600 affected
 properties. The estimated mitigation benefits based on the USACE approach are about 25% higher than those from the
 NFIP-derived depth-damage function. This discrepancy is consistent with findings from prior work (Wing et al., 2020),
 which suggest that relative flood damage cannot be well described by any central-tendency distribution, underscoring the
 300 variability and complexity of flood damage assessments and the need for a data-driven approach.

Table 4: Aggregate Benefits Across All Properties in Chatham County and Average Benefits per Household for Storm 0157

	NFIP-Derived (Without interactions)	NFIP-Derived (With interactions)	USACE
Aggregate benefits (\$1000)	30,227	33,115	40,964
Average benefits per household (\$1000)	1.94	2.12	2.65

305 **Notes:** This table presents the total benefits across all properties and the average benefits per household provided by salt
 marshes in Chatham County, Georgia, based on the simulated storm track 0157. The first column does not include
 interaction terms among water depth, number of floors, and presence of a basement, whereas the second column does. The
 third column shows the results based on the USACE depth-damage function.

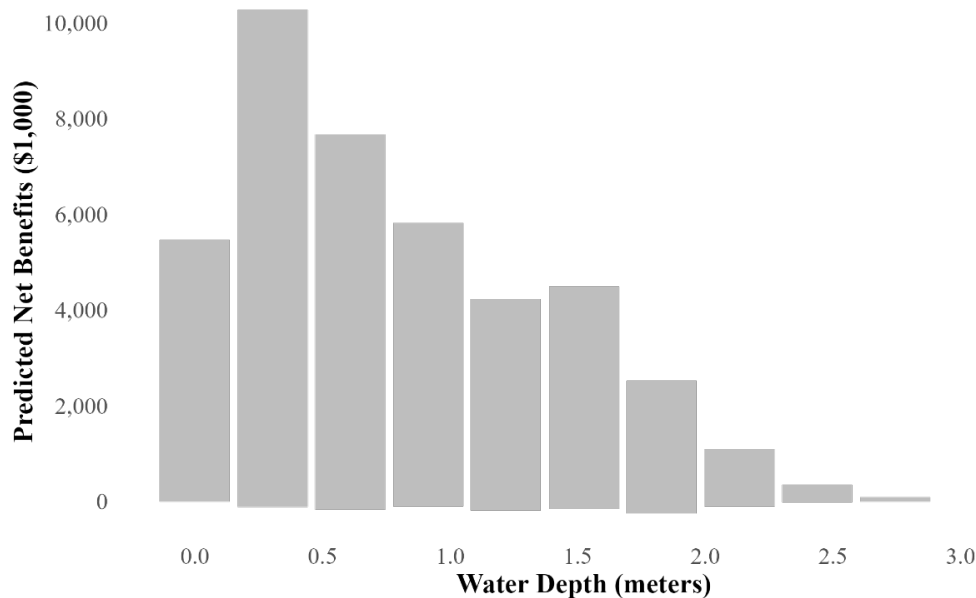
Figure 9 illustrates how the predicted avoided damage from salt marshes varies with water depth. Panel A shows the results
 based on the USACE depth-damage function, while Panel B presents the results using the NFIP-derived depth-damage
 310 function. Marshes clearly provide benefits by mitigating damage from storm-induced flooding, regardless of the depth-
 damage function used.

However, Panels A and B illustrate distinct differences in the predicted benefits based on how hydrology is translated into
 economic measures. Panel A, based on the USACE depth-damage function, shows a sharp peak in predicted benefits at
 shallow depths of 0.25-0.5 meters, followed by a steep decline, indicating that the majority of benefits are concentrated at
 315 these lower depths. In contrast, Panel B, which uses the NFIP-derived depth-damage function, presents a more symmetrical,
 normal distribution with the highest benefits occurring around 1-1.5 meters of water depth. The decline in benefits is more
 gradual, extending over a wider range of depths, and even predicting notable benefits up to 3-4 meters. This suggests that the
 NFIP-derived function anticipates more distributed benefits across various depths.

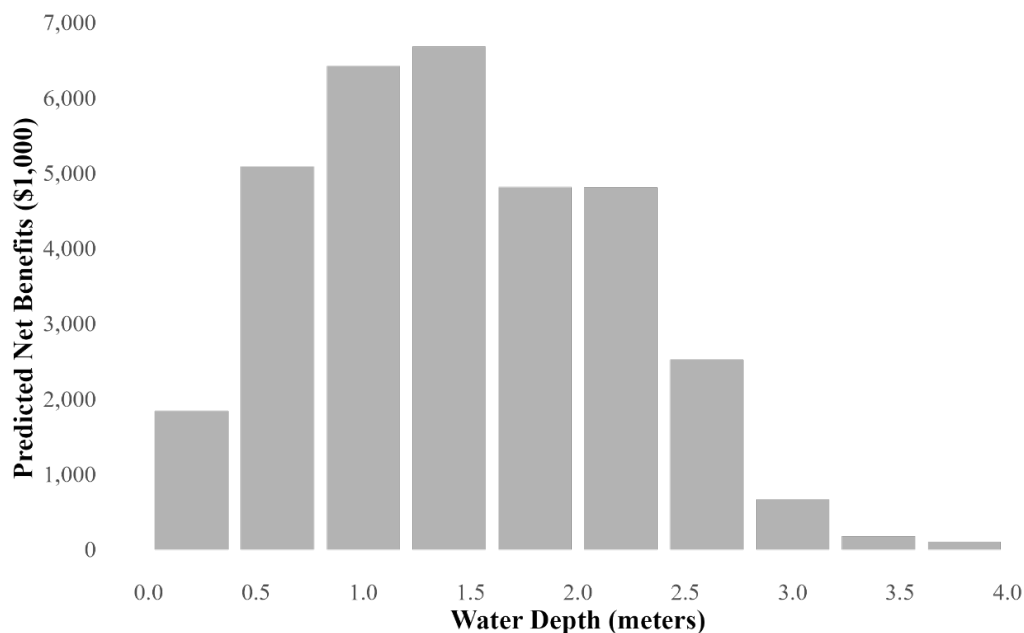


Figure 9: Histogram of Predicted Benefits of Marshes

320 (a) Based on the USACE Depth-Damage Function



(b) Based on the NFIP-derived Depth-Damage Function



325 Notes: This figure illustrates how the predicted avoided damage varies by water depth. Panel A shows the results based on the USACE depth-damage function, while Panel B presents the results using the NFIP-derived depth-damage function.



3.4 Spatial Distribution of Mitigation Benefits

Next, we examine the spatial distribution of avoided damage. Panel A and B of Figure 10 illustrate the spatial distribution of net mitigation benefits of salt marshes for properties in Chatham County, based on the USACE and NFIP-derived depth-damage functions, respectively. Properties experiencing positive benefits (i.e., salt marshes reduce flood damage) are shown from light orange to red, while those experiencing negative benefits (i.e., salt marshes increase flood damage) are highlighted in blue.

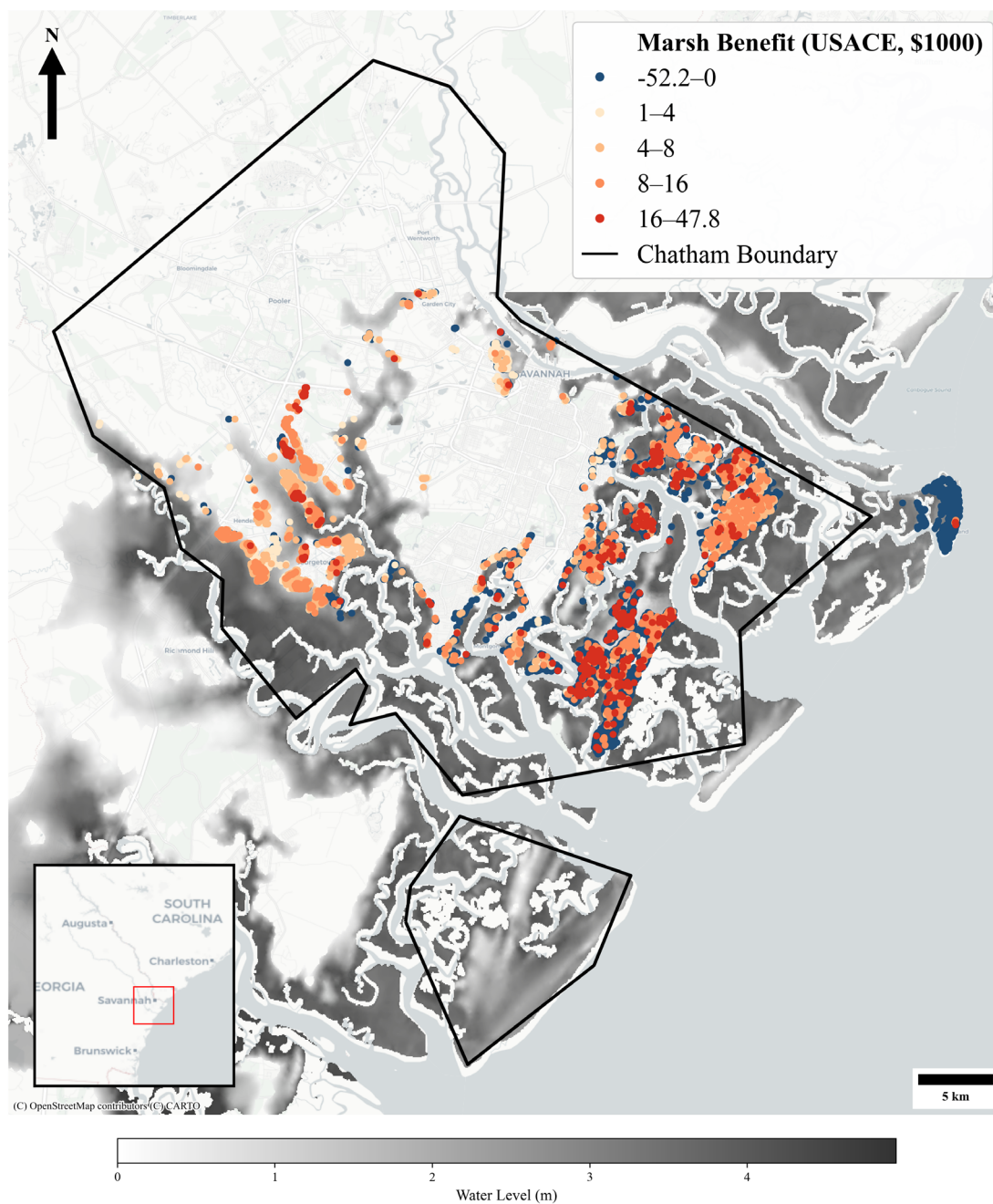
Overall, most of the effects of salt marshes are concentrated in the coastal portion of the county. Positive benefits are clustered around coastal areas with low to moderate inundation levels. In contrast, the net benefits of salt marshes for properties in the eastern corner are almost entirely negative, particularly at high inundation depths. This suggests that marshes significantly reduce but cannot eliminate flood damage under extreme inundation. It is important to note that this does not imply the ineffectiveness of marshes; rather, it signifies that marshes cannot completely nullify the full extent of flood damage.

The spatial visualization reveals some interesting patterns. Consistent with the net benefits shown in Table 4, the aggregate benefits calculated using the USACE depth-damage function are much higher than those based on the NFIP-derived depth-damage curve.



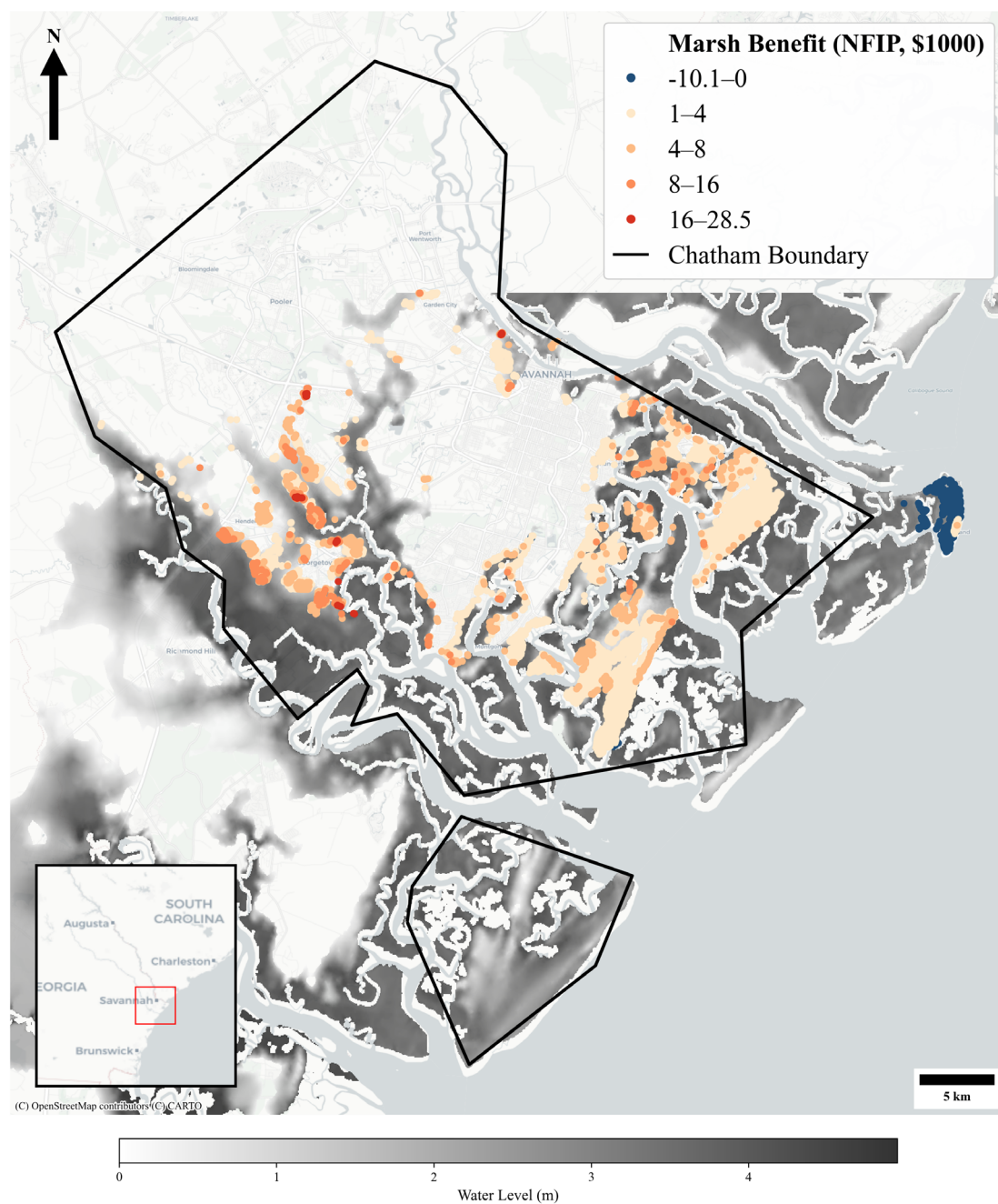
Figure 10: Spatial distribution of marshland benefits in Chatham County

345 (a) USACE depth-damage function





(b) NFIP-derived depth-damage function



350 **Notes:** This figure presents the marsh benefits for properties in Chatham County, Georgia. Marsh benefits are calculated as the difference between simulated flood damages under two scenarios: without marshes and with marshes. The simulated benefits are calculated using both depth-damage functions and the simulated inundation level. The map displays marsh benefits only for properties exposed to simulated storm inundation. Areas that appear blank relative to the NSI property map in central Chatham County indicate locations with zero modelled inundation rather than an absence of properties.



355 **3.5 Spatial Distribution of Mitigation Benefits by Socioeconomic Factors**

We further evaluate the net benefits of salt marshes across various communities by examining indicators of social and economic vulnerability, namely, racial composition and poverty rate.

Table 5 presents total and average mitigation benefits per household, categorized by quartile, for Black and White populations, with Panel A reporting results based on the USACE function and Panel B reporting results based on the NFIP-derived function. A consistent pattern emerges across both depth-damage functions: the highest mitigation benefits are most concentrated in areas with a 0% to 25% Black population (75% to 100% White population), followed by areas with approximately 50% Black population. In areas predominantly populated by Black residents (75-100%), the mitigation benefits are very low. There is a slight correlation between shares of Black residents and benefits from flood risk reduction of marsh presence (correlation = 0.3). However, given that the benefits are largest in low-Black areas, this correlation is likely driven by the middle quartile (25% - 50% Black) having moderately high benefits, while high-Black and low-Black areas diverge. This is mainly because the White population tends to locate in areas with higher real estate values, particularly along the coast, where flooding is more severe, as shown in Appendix Figure B2. These areas are also more likely to experience greater exposure to flooding events.

370 **Table 5: Aggregate and Average Mitigation Benefits per Household for Storm 0157 by Quartile of Black and White Population**

(a) USACE depth-damage function

Population Quartile		0%-25%	25%-50%	50%-75%	75%-100%
Black	Aggregated Benefit (\$1000)	17,425	7,643	14,718	1,178
	Average Benefit per Household (\$1000)	1.03	0.459	0.844	0.0729
	Weighted Average Benefit per Household (\$1000)	1.35	0.689	1.15	0.209
White	Aggregated Benefit (\$1000)	6,106	10,444	7,925	16,490
	Average Benefit per Household (\$1000)	0.348	0.622	0.476	1.01
	Weighted Average Benefit per Household (\$1000)	0.771	1.05	0.594	1.33



375 **(b) NFIP-derived depth-damage function**

	Population Quartile	0%-25%	25%-50%	50%-75%	75%-100%
Black	Aggregated Benefit (\$1000)	13,899	5,496	12,907	814
	Average Benefit per Household (\$1000)	0.818	0.330	0.740	0.050
	Weighted Average Benefit per Household (\$1000)	1.170	0.477	1.080	0.168
White	Aggregated Benefit (\$1000)	5,791	7,107	7,460	12,758
	Average Benefit per Household (\$1000)	0.330	0.423	0.448	0.783
	Weighted Average Benefit per Household (\$1000)	0.880	0.688	0.615	1.100

Notes: This table presents the total and average mitigation benefits per household, categorized by population quartile, for Black and White populations. Aggregated benefit is the sum of estimated marsh benefits across all households in each group. Average benefit is the simple mean benefit per household. Weighted average benefit is the mean benefit per household weighted by property value.

380

We also overlay the net benefits polygon of salt marshes on maps showing the racial composition and poverty rates in Chatham County to visualize correlations. The results are presented in Appendix B. Appendix Figure B1, Panel A, illustrates how the distribution of net benefits varies based on racial composition, focusing on the percentage of the Black population in census tracts. Consistent with the table results, the highest marsh benefits are concentrated on the lower to middle Black population quartiles.

385

We further calculate the total and average mitigation benefits across different poverty groups in Appendix Table B1, with the corresponding marsh benefit distribution shown in Appendix Figure B1, Panel B. The table indicates that total (aggregate) marsh mitigation benefits are higher in lower-poverty quartiles. However, the average mitigation benefit per household is relatively similar across poverty quartiles under both the USACE and NFIP depth-damage functions. Appendix Figure B1 Panel B similarly shows no clear spatial concentration in net benefits across communities with poverty levels. The correlation between marsh benefits and the poverty rate is minimal (0.028), indicating that these benefits are not strongly correlated with income levels.

390



4 Discussion

Our results demonstrate that salt marsh conservation provides substantial and spatially variable flood damage mitigation benefits in Chatham County, reducing flood damage, by approximately \$30 million to \$40 million per storm across all properties in , or about \$1,940 to \$2,650 per household. The estimated mitigation benefits based on the USACE approach are about 25% higher than those from the NFIP-derived depth-damage function. This discrepancy stems from differences in how each function translates inundation depth into economic loss: the USACE function concentrates damage at shallow depths, while the NFIP-derived function distributes damage more broadly across moderate to deeper flood depths, resulting in a lower but more empirically grounded estimate of avoided losses.

The spatial analysis of marsh benefits and socioeconomic characteristics in Chatham County shows that the avoided damage from marsh is unevenly distributed across racial groups. Marsh benefits are highest in areas with the lowest quartile of Black population share (0–25%) and lowest in areas with the highest quartile (75–100%). Consistently, benefits are largest in areas with the highest share of White residents. This pattern reflects spatial differences in flood exposure and property values: neighborhoods with larger shares of White residents tend to be located in higher-value coastal areas with greater flood exposure. As a result, these areas have more valuable properties at risk, leading to larger potential avoided damages from marsh protection.

There are some limitations in this work that warrant future investigation. While the study employs state-of-the-art hydrodynamic models at large scales, assumptions are made regarding vegetation behavior during flood events. Incorporating fine-scale physics that explicitly represent flow-vegetation interaction within the salt marsh, rather than relying on bulk friction parameterizations such as Manning's n , could improve model accuracy, and represents an important direction for future research (Temmerman et al., 2005). Additionally, this work only considered the 1% AEP coastal flood event. While the 1% AEP is a main driver of policy and planning in the US, evaluating a broader range of flood probabilities would provide additional insight into the role of coastal marsh vegetation in flood mitigation.

Furthermore, the depth–damage function approach assumes that inundation depth and building structure are the primary determinants of economic loss, while other factors, such as flood duration, flow velocity, salinity, and variation in building materials, are not fully observable in our data and therefore not explicitly modeled. As noted by Porter et al. (2023), different types of flooding may exhibit distinct depth–damage relationships, for example, riverine versus coastal flooding. The use of insurance claims data may also introduce measurement error or selection bias, as reported damages may reflect (unobserved) heterogeneity of coverage limits, deductible structures, reporting behavior, and post-disaster assistance rules, in addition to physical losses. Finally, functions estimated from historical events may not fully capture damage processes under future climate conditions, particularly in the presence of compound flooding.

Despite these considerations, the empirical advantages of our approach are substantial. The estimates are based on observed property-level outcomes across multiple storms and geographic areas, allowing us to capture real-world variation in flood exposure and damages. The large sample size and consistent modeling framework reduce reliance on stylized assumptions



and provide internally consistent estimates of avoided losses. Moreover, because the damage function is estimated directly from observed claims data, it offers a data-driven alternative to the conventional USACE depth–damage functions and can serve as a practical complement in settings where local empirical calibration is feasible. Taken together, the results provide a careful and policy-relevant assessment of flood damage and the protective role of salt marshes, offering credible evidence to inform resilience planning and adaptation decisions.

5 Conclusions

Flooding is one of the costliest natural disasters affecting millions of people in the US, especially in coastal regions. Nature-based solutions, such as coastal habitats, are gaining popularity among the federal government and many US states and cities as a cost-effective way to reduce wave height and energy, thereby mitigating flood risks. State and local governmental agencies, along with non-governmental organizations, have implemented regulations and programs to promote the development of green infrastructure, including salt marshes, a critical type of coastal habitat.

Georgia, which harbors approximately one-third of the total salt marsh area on the U.S. eastern coast, has a long history of coastal protection through the Coastal Marshlands Protection Act. The findings of this study support continued investment in salt marsh conservation as an effective nature-based strategy for flood mitigation. Our analysis finds that salt marshes could reduce flood damage by around \$2,000 per household for a simulated storm that is typical of our study area of Chatham County, Georgia, which surrounds the City of Savannah. This is a non-trivial amount, compared to the average per-household flood damage recorded in the NFIP claim data of \$27,177.

More broadly, our findings provide concrete empirical evidence of the monetary benefits of salt marshes in mitigating flood damage, facilitating the integration of these benefits into benefit-cost calculations and informing decision-making across the United States and globally. Building on this empirical foundation, our approach combines hydrodynamic modeling with empirically estimated damage functions to offer a practical tool that can be applied to coastal regions beyond our case study. Such integrated analysis can help policymakers evaluate the role of green infrastructure as part of broader strategies to improve resilience to coastal flood risks. While salt marsh alone will not be sufficient to protect homes from flood events, they represent a viable part of an adaptation strategy for many coastal communities.

5 Appendices

Appendix A

Appendix A reports additional results for an alternative storm track (1313).



Table A1: USACE SACS Storm Track Parameters for Storm 1313.

Storm ID	Storm Heading (deg)	Central Pressure Deficit (hPa)	Radius of Maximum Winds (km)	Translational Speed (km/h)
1313	20	88	65.5	34.7

Table A2. Aggregate and Average Per-Household Mitigation Benefits for Storms 1313

Storm	Model	Aggregate (\$1,000)	Avg. per HH (\$1,000)
1313	NFIP w/o interactions	18,889	1.42
	NFIP with interactions	20,488	1.54
	USACE	26,587	2.02

460 **Notes:** This table reports the total and per-household benefits of salt marshes in Chatham County, Georgia, estimated from three models across the simulated storm track 1313

Appendix B

Appendix B provides additional distributional analysis of marsh mitigation benefits across socioeconomic groups.

Table B1. Aggregate and Average Mitigation Benefits per Household for Storm 0157 by Poverty Quartile

465 (a) USACE depth-damage function

Poverty Quartile	0%-25%	25%-50%	50%-75%	75%-100%
Aggregated Benefit (\$1000)	15,650	15,252	5,582	4,428
Average Benefit per Household (\$1000)	2.960	2.240	2.970	2.980
Weighted Average Benefit per Household (\$1000)	1.220	1.250	0.438	0.808

(b) NFIP depth-damage function

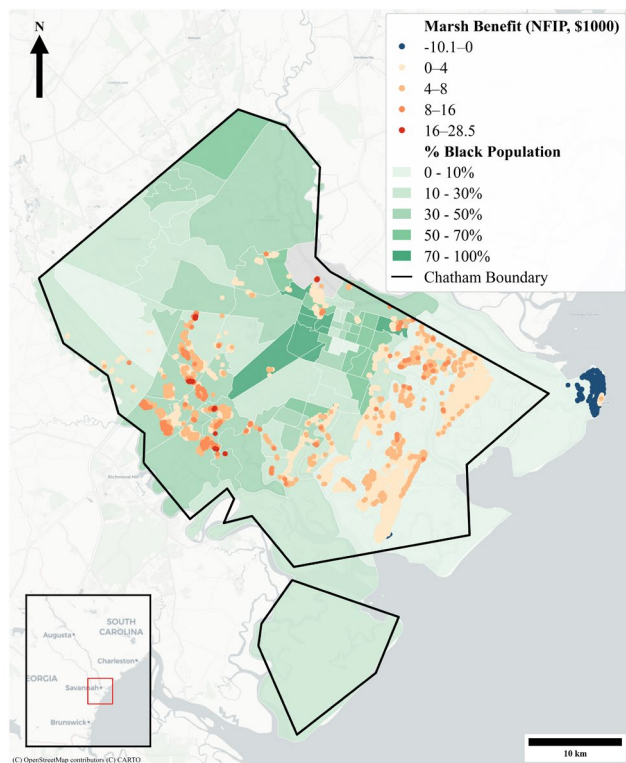
Poverty Quartile	0%-25%	25%-50%	50%-75%	75%-100%
Aggregated Benefit (\$1000)	12,797	12,977	3,883	3,210
Average Benefit per Household (\$1000)	2.40	1.890	2.060	2.140
Weighted Average Benefit per Household (\$1000)	1.040	1.100	0.297	0.588

470 **Notes:** This table reports total and average marsh mitigation benefits per household, grouped by quartiles of the poverty rates. Quartiles are based on the observed distribution of poverty rates in Chatham County at the census tract level, with cut-off points at 0.000, 0.040, 0.088, 0.168, and 0.652. The top quartile (“75–100%”), therefore, corresponds to the 25% of tracts with the highest poverty rates (ranging from 16.8%–65.2%), rather than literal poverty rates between 75% and 100%

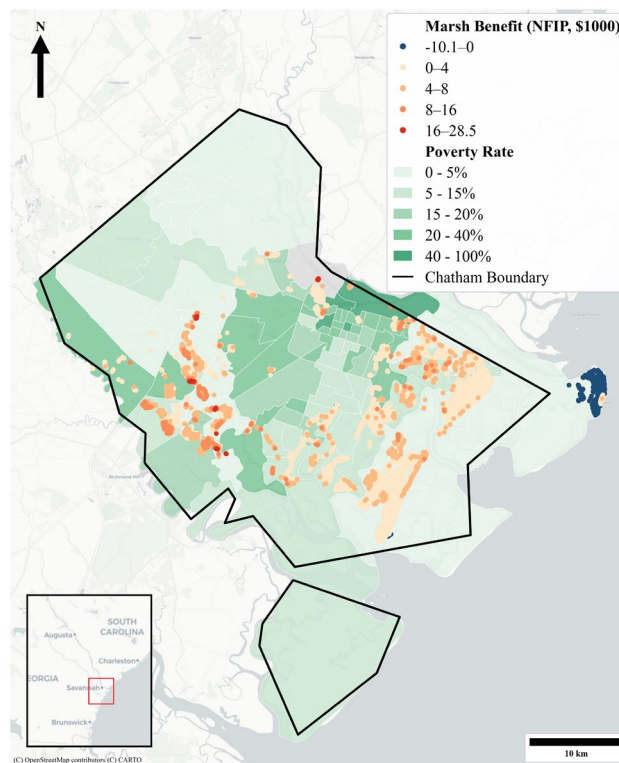


Figure B1. Spatial Distribution of Marsh Benefits (NFIP method) by Socioeconomic Factors

(a) Marsh Benefits and Race



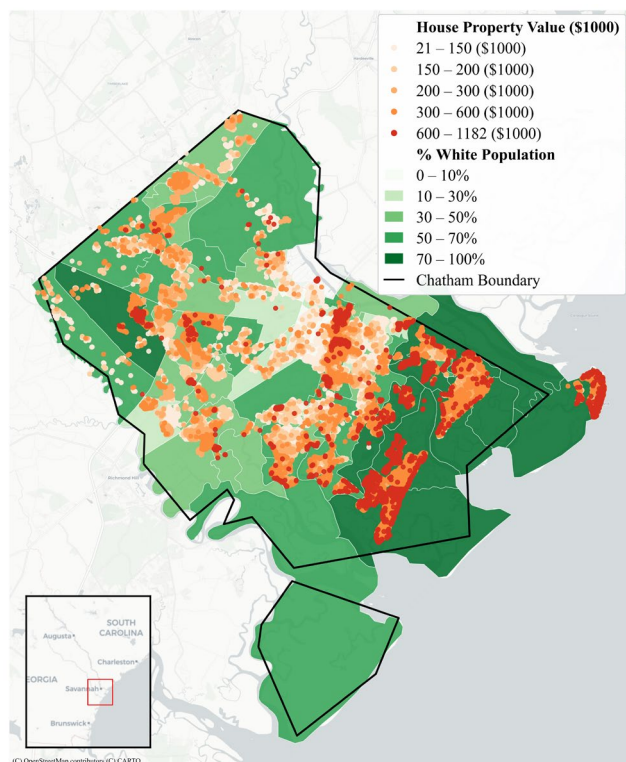
(b) Marsh Benefits and Poverty Rates



475 **Notes:** Panel A illustrates how the distribution of net benefits varies based on racial composition, focusing on the percentage of the Black population in census tracts. Panel B illustrates the differences in net benefits across communities with varying poverty levels.



Figure B2. Spatial Distribution of House Property Value and Race in Chatham County



480 Notes: This map illustrates the spatial relationship between residential property values and the White population across Chatham County. The color of each polygon represents the percentage of White residents, with darker green tones indicating higher proportions. Overlaid points represent house real estate values (in \$1,000s), ranging from light orange (lower values) to deep red (higher values). The Chatham County boundary is outlined in black.

Appendix C

485 To ensure consistency between the USACE depth-damage function and our estimated depth-damage function using NFIP data, and to facilitate comparisons between the two methods, we further restrict our sample in the following ways.

First, we limit the sample to single-family housing residential buildings with up to three stories. We also remove observations where relative damage, our main variable of interest, fall outside of the logical range [0,1] or either building damage or property value is missing. We further limit the sample to water depth not exceeding eight feet, a range where the majority of records are reliably reported in feet rather than inches. To be consistent with the result under hydrodynamic simulations, we then convert the unit of water depth into meter.

490 Second, we reclassify the basement structures in the NFIP claims data, originally categorized as 0 (none), 1 (finished basement/enclosure), 2 (unfinished basement/enclosure), 3 (crawl space), and 4 (subgrade crawl space), into two categories, with 1 indicating finished basements and 0 indicating no basement. Specifically, properties with finished and unfinished



495 basement/enclosure, as well as a crawlspace and subgrade crawlspace are categorized as having a basement, those without
are categorized as not having a basement.

Note that about 70% of the observations in the raw NFIP claims have missing values for basement type. To address this, we
take the following steps. First, buildings identified as “elevated” structures (*elevatedBuildingIndicator* = 1) are
classified as having no basement, as elevated buildings are defined in NFIP datasets as structures raised above ground level
500 on pilings, columns, shear walls, or perimeter walls and therefore do not contain basements. Second, Buildings with
elevation certificates indicating “basement or crawlspace” are categorized as having a basement. The elevation code include
A (Basement/Subgrade Crawlspace), B (Fill/Crawlspace), C (Piles/Columns with enclosure), D (Piles/Columns without
enclosure), E (Slab on grade), among others. Buildings associated with codes A or B are categorized as having a basement or
crawlspace. Lastly, we incorporate the “location of contents” variable, which records the location of insured contents. If the
505 variable shows contents in any underground space, such as basement or crawlspace only (code 1) or basement/crawlspace
and above-ground levels (code 2), those buildings are also classified as having a basement. After these steps, the percentage
of missing values for the basement type decreases to 12.95%.

Appendix D

To test the robustness of our NFIP main results estimated using fractional logistic models, we also fit beta regression models
510 where the dependent variable, the relative damage proportion, is modeled with a logit link under the beta distribution. Unlike
linear probability models, beta regression accounts for a bounded outcome and allows the conditional variance to depend on
the mean. This provides an alternative way of modeling relative damage and allows us to confirm that our results are not
sensitive to model choice. The model is specified as:

$$\text{logit}(\mu_i) = \beta_0 + \beta_1 \text{WaterDepth}_i + \beta_2 \text{Floors}_i + \beta_3 \text{Basement}_i, \quad (\text{D1})$$

515 where $\mu_i = E(y_i|X_i)$ and $y_i \sim \text{Beta}(\mu_i\phi, (1 - \mu_i)\phi)$

Here, y_i denote the relative damage (building damage divided by property value) and $\phi > 0$ is the precision parameter.
Larger values of ϕ indicate less dispersion of damages around the mean. *WaterDepth_i* is the flood inundation depth
measured in meter. *Floors_i* shows the number of floors, and *Basement_i* equals 1 if the property has a basement, 0
otherwise.

520 The interaction terms between *WaterDepth_i*, *Basement_i*, and *Floors_i* are included in a separate model to account for the
heterogeneous effect of water depth on relative damage by building structures. Because the claims data contain some
properties with either no damage or total loss, we use an extended version of the beta model that incorporates an exceedence
parameter ν to handle boundary values.

Table D1 presents the results. Across all specifications, the findings are consistent with the results from the fractional logistic
525 models. In both approaches, flood inundation depth is strongly and positively associated with the relative damage, with



coefficients of similar magnitude. The consistency of these estimates confirms the robustness of main results.

Table D1. Beta Regression Results

	(1)	(2)	(3)	(4)
Water Depth (m)	0.262*** (0.005)	0.280*** (0.005)	0.296*** (0.005)	0.468*** (0.013)
Number of Floors		-0.121*** (0.003)	-0.066*** (0.003)	-0.029*** (0.006)
With Basement			-0.228*** (0.006)	-0.015 (0.027)
Interaction with “Number of Floors” and “With Basement”	No	No	No	Yes
ϕ	2.386*** (0.007)	2.412*** (0.008)	2.431*** (0.008)	2.437*** (0.008)
ν (log)	-7.534*** (0.028)	-7.516*** (0.028)	-7.508*** (0.028)	-7.510*** (0.028)
Observations	209124	209124	209124	209124
Log.Lik.	119352.118	120287.398	121086.044	121321.685

Notes: This table presents the estimation results of the NFIP-derived depth-damage function using a beta regression. Robust standard errors are in parentheses. Significance denoted by * $p < 0.1$; ** $p < 0.05$; *** $p < 0.01$.



Code and data availability

The FEMA National Flood Insurance Program (NFIP) claims data used in this study are publicly available through the FEMA OpenFEMA portal (<https://www.fema.gov/openfema-data-page/fima-nfip-redacted-claims-v2>, last access: 4
535 September 2024). USACE depth–damage functions were obtained from publicly available technical documentation referenced in the manuscript. The 2019 parcel-level data for Chatham County, Georgia were obtained from the Savannah Area GIS open data portal (<https://data-sagis.opendata.arcgis.com/datasets/SAGIS::parcel-digest-2019-2/about>, last access: 26 February 2026). This dataset may no longer be available at this URL; interested researchers may contact the Chatham County–Savannah Area GIS office directly for access.

540 Custom scripts used for data processing, statistical modeling, and figure production are available from the corresponding author upon reasonable request and will be archived in a public repository prior to final publication. Processed datasets required to reproduce the figures and analyses will be deposited in a FAIR-aligned repository with a DOI upon acceptance.

Author contributions

Xinyu Zeng: Writing – original draft, Writing – review & editing, Visualization, Validation, Software, Formal analysis, Data curation, Investigation, Methodology, Conceptualization. **Dede Long:** Writing – original draft, Writing – review & editing, Visualization, Methodology, Formal analysis, Conceptualization. **Yukiko Hashida:** Writing – review & editing, Supervision, Project administration, Resources, Funding acquisition, Methodology, Conceptualization. **Matthew V. Bilskie:** Writing – review & editing, Validation, Investigation, Methodology, Resources

Competing interests

550 The authors declare that they have no conflict of interest.

Financial support

This work was supported by Georgia Sea Grant and Marine Extension Award #NA22OAR4170116.

References

Arkema, K. K., Guannel, G., Verutes, G., Wood, S. A., Guerry, A., Ruckelshaus, M., Kareiva, P., Lacayo, M., and Silver, J.
555 M.: Coastal habitats shield people and property from sea-level rise and storms, *Nature Clim Change*, 3, 913–918, <https://doi.org/10.1038/nclimate1944>, 2013.



- Battjes, J. A. and Janssen, J. P. F. M.: Energy Loss and Set-Up Due to Breaking of Random Waves, in: Coastal Engineering 1978, 16th International Conference on Coastal Engineering, 569–587, <https://doi.org/10.1061/9780872621909.034>, 1978.
- 560 Bolster, P.: Saving the Georgia Coast: A Political History of the Coastal Marshlands Protection Act, University of Georgia Press, 369 pp., 2020.
- Castagno, K. A., Tomiczek, T., Shepard, C. C., and et al: Resistance, resilience, and recovery of salt marshes in the Florida Panhandle following Hurricane Michael, Scientific Reports, 11, 20381, <https://doi.org/10.1038/s41598-021-99779-8>, 2021.
- 565 Cavaleri, L. and Rizzoli, P. M.: Wind wave prediction in shallow water: Theory and applications, Journal of Geophysical Research: Oceans, 86, 10961–10973, <https://doi.org/10.1029/JC086iC11p10961>, 1981.
- Chatham County: Resilient Chatham County: Resilience program hub: <https://www.chathamcountyga.gov/OurCounty/Resiliency>, last access: 3 February 2026.
- Chatham County Department of Engineering: Flood Facts for Unincorporated Chatham County Residents, 2025.
- 570 Costanza, R., Anderson, S. J., Sutton, P., Mulder, K., Mulder, O., Kubiszewski, I., Wang, X., Liu, X., Pérez-Maqueo, O., Luisa Martinez, M., Jarvis, D., and Dee, G.: The global value of coastal wetlands for storm protection, Global Environmental Change, 70, 102328, <https://doi.org/10.1016/j.gloenvcha.2021.102328>, 2021.
- Cutter, S. L., Emrich, C. T., Gall, M., and Reeves, R.: Flash Flood Risk and the Paradox of Urban Development, Natural Hazards Review, 19, 05017005, [https://doi.org/10.1061/\(ASCE\)NH.1527-6996.0000268](https://doi.org/10.1061/(ASCE)NH.1527-6996.0000268), 2018.
- 575 Davis, S. A. and Skaggs, L. L.: Catalog of residential depth-damage functions used by the army corps of engineers in flood damage estimation, U.S. Army Engineer Institute for Water Resources, Fort Belvoir, VA, 1992.
- Dietrich, J. C., Zijlema, M., Westerink, J. J., Holthuijsen, L. H., Dawson, C., Luetlich, R. A., Jensen, R. E., Smith, J. M., Stelling, G. S., and Stone, G. W.: Modeling hurricane waves and storm surge using integrally-coupled, scalable computations, Coastal Engineering, 58, 45–65, <https://doi.org/10.1016/j.coastaleng.2010.08.001>, 2011.
- 580 Fagherazzi, S., Mariotti, G., Wiberg, P. L., and McGLATHERY, K. J.: Marsh collapse does not require sea level rise, Oceanography, 26, 70–77, 2013.



- Farber, S.: The value of coastal wetlands for protection of property against hurricane wind damage, *Journal of Environmental Economics and Management*, 14, 143–151, [https://doi.org/10.1016/0095-0696\(87\)90012-X](https://doi.org/10.1016/0095-0696(87)90012-X), 1987.
- FEMA: *Guidance for Flood Risk Analysis and Mapping: Flood Risk Assessments*, Federal Emergency Management Agency, 2020.
- 585 Ferrario, F., Beck, M. W., Storlazzi, C. D., Micheli, F., Shepard, C. C., and Airolidi, L.: The effectiveness of coral reefs for coastal hazard risk reduction and adaptation, *Nat Commun*, 5, 3794, <https://doi.org/10.1038/ncomms4794>, 2014.
- Gedan, K. B., Silliman, B. R., and Bertness, M. D.: Centuries of Human-Driven Change in Salt Marsh Ecosystems, *Annual Review of Marine Science*, 1, 117–141, <https://doi.org/10.1146/annurev.marine.010908.163930>, 2009.
- 590 Guannel, G., Ruggiero, P., Faries, J., Arkema, K., Pinsky, M., Gelfenbaum, G., Guerry, A., and Kim, C.-K.: Integrated modeling framework to quantify the coastal protection services supplied by vegetation, *Journal of Geophysical Research (Oceans)*, 120, 324–345, <https://doi.org/10.1002/2014JC009821>, 2015.
- Horn, D. P. and Webel, B.: *Introduction to the National Flood Insurance Program (NFIP)*, Congressional Research Service, Washington, DC, 2025.
- 595 Komen, G. J., Hasselmann, S., and Hasselmann, K.: On the existence of a fully developed wind-sea spectrum, *Journal of Physical Oceanography*, 14, 1271–1285, [https://doi.org/10.1175/1520-0485\(1984\)014%253C1271:OTEOAF%253E2.0.CO;2](https://doi.org/10.1175/1520-0485(1984)014%253C1271:OTEOAF%253E2.0.CO;2), 1984.
- Kousky, C., Kunreuther, H., Lingle, B., and Shabman, L.: *Structure of the Residential Flood Insurance Market, Resources for the Future*, 2023.
- 600 Leonardi, N. and Fagherazzi, S.: Effect of local variability in erosional resistance on large-scale morphodynamic response of salt marshes to wind waves and extreme events, *Geophysical Research Letters*, 42, 5872–5879, <https://doi.org/10.1002/2015GL064730>, 2015.
- Luetlich, R. A. and Westerink, J. J.: *Formulation and Numerical Implementation of the 2D/3D ADCIRC Finite Element Model Version 44.XX*, U.S. Army Corps of Engineers, 2004.



- 605 Madsen, O. S., Poon, Y.-K., and Graber, H. C.: Spectral Wave Attenuation by Bottom Friction: Theory, in: Coastal Engineering 1988, 21st International Conference on Coastal Engineering, 492–504, <https://doi.org/10.1061/9780872626874.035>, 1988.
- Massey, T., Massey, M., Provost, L., Bryant, M., Hesser, T., Tritinger, A., Dillon, S., Goertz, J., Ding, Y., and Nadal-Caraballo, N.: South Atlantic South Atlantic Coastal Study (SACS) calibration and validation of the Coastal Storm Modeling System (CSTORM-MS) for water levels and waves : Part 2. South Atlantic Coast domain, Engineer
610 Research and Development Center (U.S.), <https://doi.org/10.21079/11681/49896>, 2025.
- Möller, I., Kudella, M., Rupprecht, F., Spencer, T., Paul, M., van Wesenbeeck, B. K., Wolters, G., Jensen, K., Bouma, T. J., Miranda-Lange, M., and Schimmels, S.: Wave attenuation over coastal salt marshes under storm surge conditions, Nature Geosci, 7, 727–731, <https://doi.org/10.1038/ngeo2251>, 2014.
- 615 Morton, R. A. and Barras, J. A.: Hurricane impacts on coastal wetlands: A half-century record of storm-generated features from southern Louisiana, Journal of Coastal Research, 27, 27–43, <https://doi.org/10.2112/JCOASTRES-D-10-00185.1>, 2011.
- Narayan, S., Beck, M. W., Wilson, P., Thomas, C. J., Guerrero, A., Shepard, C. C., Reguero, B. G., Franco, G., Ingram, J. C., and Trespalacios, D.: The Value of Coastal Wetlands for Flood Damage Reduction in the Northeastern USA,
620 Sci Rep, 7, 9463, <https://doi.org/10.1038/s41598-017-09269-z>, 2017.
- NOAA: Economics and demographics: Almost 40% live on the coast: <https://coast.noaa.gov/states/fast-facts/economics-and-demographics.html>, last access: 3 March 2026.
- Papke, L. E. and Wooldridge, J. M.: Econometric methods for fractional response variables with an application to 401(k) plan participation rates, J. Appl. Econ., 11, 619–632, [https://doi.org/10.1002/\(SICI\)1099-1255\(199611\)11:6%253C619::AID-JAE418%253E3.0.CO;2-1](https://doi.org/10.1002/(SICI)1099-1255(199611)11:6%253C619::AID-JAE418%253E3.0.CO;2-1), 1996.
625
- Porter, J. R., Marston, M. L., Shu, E., Bauer, M., Lai, K., Wilson, B., and Pope, M.: Estimating Pluvial Depth–Damage Functions for Areas within the United States Using Historical Claims Data, Nat. Hazards Rev., 24, 04022048, <https://doi.org/10.1061/NHREFO.NHENG-1543>, 2023.



- 630 Rezaie, A. M., Loerzel, J., and Ferreira, C. M.: Valuing natural habitats for enhancing coastal resilience: Wetlands reduce property damage from storm surge and sea level rise, *PLOS ONE*, 15, e0226275, <https://doi.org/10.1371/journal.pone.0226275>, 2020.
- Shepard, C. C., Crain, C. M., and Beck, M. W.: The Protective Role of Coastal Marshes: A Systematic Review and Meta-analysis, *PLOS ONE*, 6, e27374, <https://doi.org/10.1371/journal.pone.0027374>, 2011.
- Spalding, M. D., McIvor, A. L., Beck, M. W., Koch, E. W., Möller, I., Reed, D. J., Rubinoff, P., Spencer, T., Tolhurst, T. J., 635 Wamsley, T. V., van Wesenbeeck, B. K., Wolanski, E., and Woodroffe, C. D.: Coastal Ecosystems: A Critical Element of Risk Reduction, *Conservation Letters*, 7, 293–301, <https://doi.org/10.1111/conl.12074>, 2014.
- Sun, F. and Carson, R. T.: Coastal wetlands reduce property damage during tropical cyclones, *Proc Natl Acad Sci USA*, 117, 5719–5725, <https://doi.org/10.1073/pnas.1915169117>, 2020.
- Taylor, C. A. and Druckenmiller, H.: Wetlands, Flooding, and the Clean Water Act, *American Economic Review*, 112, 640 1334–1363, <https://doi.org/10.1257/aer.20210497>, 2022.
- Temmerman, S., Bouma, T. J., Govers, G., Wang, Z. B., De Vries, M. B., and Herman, P. M. J.: Impact of vegetation on flow routing and sedimentation patterns: Three-dimensional modeling for a tidal marsh, *J. Geophys. Res.*, 110, 2005JF000301, <https://doi.org/10.1029/2005JF000301>, 2005.
- U.S. Army Corps of Engineers: South Atlantic coastal study: Engineering appendix, U.S. Army Corps of Engineers, South 645 Atlantic Division, 2022.
- USACE: National Structure Inventory: 2022 Technical Documentation, U.S. Army Corps of Engineers, Hydrologic Engineering Center, 2022.
- Walters, D. C. and Kirwan, M. L.: Optimal hurricane overwash thickness for maximizing marsh resilience to sea level rise, *Ecology and Evolution*, 6, 2948–2956, <https://doi.org/10.1002/ece3.2024>, 2016.
- 650 Westerink, J. J., Luettich, R. A., Feyen, J. C., Atkinson, J. H., Dawson, C., Roberts, H. J., and Pourtaheri, H.: A basin-to-channel-scale unstructured grid hurricane storm surge model applied to southern Louisiana, *Monthly Weather Review*, 136, 833–864, <https://doi.org/10.1175/2007MWR1946.1>, 2008.



- Wing, O. E. J., Pinter, N., Bates, P. D., and Kousky, C.: New insights into US flood vulnerability revealed from flood insurance big data, *Nat Commun*, 11, 1444, <https://doi.org/10.1038/s41467-020-15264-2>, 2020.
- 655 Wing, O. E. J., Lehman, W., Bates, P. D., Sampson, C. C., Quinn, N., Smith, A. M., Neal, J. C., Porter, J. R., and Kousky, C.: Inequitable patterns of US flood risk in the Anthropocene, *Nat. Clim. Chang.*, 12, 156–162, <https://doi.org/10.1038/s41558-021-01265-6>, 2022.
- van Zelst, V. T. M., Dijkstra, J. T., van Wesenbeeck, B. K., Eilander, D., Morris, E. P., Winsemius, H. C., Ward, P. J., and de Vries, M. B.: Cutting the costs of coastal protection by integrating vegetation in flood defences, *Nat Commun*, 12, 6533, <https://doi.org/10.1038/s41467-021-26887-4>, 2021.
- 660